International Journal of Latest Engineering Research and Applications (IJLERA) ISSN: 2455-7137

Volume –05, Issue – 03, March 2020, PP – 31-46

Summary of mathematical models in fundamental cases of breakdowns in rotary machines by detection of vibration signals

B. Fraga De Cal

Renewable Energy MSc. (Queen Mary University of London)
Mechanical Engineer MSc. (Antonio de Nebrija University, Spain)
Mechanical Engineer Designer, Energy & Sustainability
Ph D. Student, A Coruña University, Spain

Abstract: The actual maintenance predictive in rotative machinery presents a trend based on information from online monitoring vibration systems. Some specific malfunction symptoms supported by simple mathematical models are given, which include unbalance, rotor to stator rubbing, misalignment, fluid induced vibrations, Synchronous Dynamic Stiffness. Applications of synchronous perturbation testing, used for identification of basic dynamic characteristics of machinery are presented. The purpose of this paper is to present simple mathematical models that describe fundamental cause/effect/response relationships for several most important vibration related machinery malfunctions is adopted. In all models the modal approach is adopted, and mainly the first lateral mode of the rotor is considered. These mathematical models will be essential for the implementation of intelligent expert systems that detect and recommend the actions to be taken in case of the presence of breakdowns.

Keywords: Rotor dynamics; fundamental breakdown, mathematical models, vibration signals.

I. Introduction

Modern industrial processes demand operation over a wide range of the variables involved. In all cases it is economically favourable to evaluate the on-stream mechanical condition of the process on line machinery. In the search of parameters to accurately access mechanical condition, the measurement of on-line machine vibration characteristics has consistently proven to be powerful tool.

Successful vibration measurement and analysis requires an intimate familiarity with the types of measurements, transducers characteristics and application, plus the capabilities and limitations of the diagnostic instrumentation.

The most current data presentation techniques are: i) Steady State Data: Time Domain Analysis (rotor displacement, shaft orbit) or in the time domain or in the frequency domain (spectrum analysis); ii) Transient Data: Cascade Spectrum analysis, Bodé/Polar diagrams, Extended Time Domain, Summary/Trend Plots.

The value that the suppliers of instrumentation for condition monitoring provide to machine users evolved considerably during the last decade. The early instruments offered by de instrumentation suppliers were limited to the readings of the vibration levels in terms of the vibration overall amplitude.

On line experts' systems are playing a progressively more important role in industry because they can serve as vehicles for the distribution of the high-level engineering expertise to a wide range of users. Expert systems can considerably improve access to the knowledge and experience of human experts, resulting in performance, cost and quality improvements. [1]

The "International Organization for Standard» (ISO)" [2] dictates the corresponding use of the transducers, accelerometers, velocity or the eddy current proximity. The set of transducers installed on a machine is the heart of the now sophisticated monitoring. These systems include data acquisition and processing hardware and software. Two transducers must be installed in orthogonal position, according to the x-y axes, and another third for phase reference.

"Modal" transducers installed at the other axial locations should supplement the basic rotor lateral transducer measurements. With these transducers, the high-speed rotor modal shape can be satisfactorily identified. [3]. The information from "modal" transducers is also successfully used for observed "Synchronous Dynamic Stiffness" [4].

The lateral characteristics of rotor supporting structures usually exhibit some degree of anisotropy, mainly in stiffness. This results in "1ω" (rotary speed) and other frequency response elliptical orbits, and in slightly different values of natural frequencies for pairs of orthogonal lateral modes, shown in "1ω" Bodé and Polar plots as "split resonances"

Often unobserved, but the torsional vibration is very important. The machine operators frequently do not realize the existence of rotor vibrations, which are quiet, and do not propagate to the other elements of the machine. Only dedicated transducers can detect the torsional vibrations. The torsional activity usually accompanies the lateral vibration as the simple mechanism of energy transfer is through most common, even residual malfunctions such as unbalance and misalignment. If the machine operating speed is higher than the rotor torsional mode natural frequency, the "quiet" torsional vibration may a cause a lot of damage, causal significantly to rotor overall stress during each start up and shutdown.

To achieve the basic characteristic of the machine such as geometry, weight, clearance, etc. and the fundamental dynamic behaviour during its operation, the process and vibration should be acquired as soon as during acceptance and commissioning tests. This process provides baseline data for insight to:

- The natural frequencies of the system and mode shapes, particularly those of the machine rotor.
- The effective damping of the system.
- The margin of safety against instability of the rotor system.
- The load to vibration interaction.
- Acceptable vibration limits.
- Dynamic stiffness of de system.

Analytic models of the machine dynamic behaviour are of great value in diagnostics procedures. The analytical and testing baseline information is necessary for comparing the machine´s previous and present condition when a machine malfunction occurs. Many of the reference data and operational requirements of the process, as well as a complete machine loss profile, must be provided by the manufacturer.

II. Synchronous Dynamic Stiffness

The matrix of system synchronous dynamic stiffness is an inverse of the influence vector matrix, equation(1. The transfer function routinely generated during balancing procedures, and unfortunately underestimated as useful information. The analysis of the vibration response of a machine identifies the mechanical characteristics of the machine, and is only the relationship between the forces acting on the machine and its dynamic stiffness, in which using a weight added to the rotor that rotates with the speed of the machine will be:

$$\vec{R}(synchronous\ response) = \frac{\vec{F}}{\vec{K}} = \frac{(unbalanced\ forced)}{(Synchronous\ Dynamic\ Stiffness)}$$

This means that the vibration response can be increased, by the appearance of an anomalous disruptive force, or by the decrease in mechanical restraint.

The equations (2 y (3 correspond to the measurement in the two planes studied, taking into account the incorporation of the determined weights, and which produce the added forces $\vec{F}_{1c}$ y $\vec{F}_{2c}$ respectively:

1. First rotation:

$$\begin{aligned} INPUT\ Unbalanced forces unknown \ \Rightarrow\ & \frac{Plane\ 1}{Plane\ 2}[\underline{F}_1\ \underline{F}_2\ ] \\ \rightarrow\ & [\ \underline{H}\ ] \\ =\ & [\underline{H}_{11}\ \underline{H}_{12}\ \underline{H}_{21}\ \underline{H}_{22}\ ]_{\smile} \ = vectors of influence \\ =\ & [dynamics tiffness]^{-1} \ \rightsquigarrow rotor transfer function \\ \rightarrow\ & [\underline{A}_{10}\ \underline{A}_{20}\ ] \ \rightsquigarrow OUTPUT\ vibration response \end{aligned} \tag{1}$$

2. Calibration with known weight in the plane "1" (force $\overrightarrow{F}_{1C}$):

$$2.-Plane\ 1\ INPUT\ \left(Force\underline{F}_{1c}\right) \Rightarrow \left[\underline{F}_1\ \underline{F}_2\ \right] + \left[\underline{F}_{1c}\ 0\ \right] \ \rightarrow\ [\ \underline{H}\ ] \ \rightarrow \left[\underline{A}_{11}\ \underline{A}_{21}\ \right] \rightsquigarrow^{vibration\ response} \tag{2}$$

3. Calibration with known weight in the plane "2" (force $\overrightarrow{F}_{2C}$):

$$3.-Plane\ 2\ INPUT\ \left(Force\ \underline{F}_{2c}\right) \Rightarrow \left[\underline{F}_1\ \underline{F}_2\ \right] + \left[0\ \underline{F}_{2c}\ \right] \ \rightarrow\ [\ \underline{H}\ ] \ \rightarrow \left[\underline{A}_{12}\ \underline{A}_{22}\ \right] \rightsquigarrow^{vibration\ response} \tag{3}$$

4. The equation that identifies the unbalance results:

$$\begin{aligned} \left[\underline{F}_1\ \underline{F}_2\ \right] = & \left[-\underline{F}_{1C}\ 0\ 0\ -\underline{F}_{2c}\ \right]\left[\underline{A}_{10}\ -\ \underline{A}_{11}\ \underline{A}_{10}\ -\underline{A}_{12}\ \underline{A}_{20}\ -\ \underline{A}_{11}\ \underline{A}_{20}\ -\underline{A}_{22}\ \right]^{-1}{}_{\smile} \left[\underline{A}_{10}\ \underline{A}_{20}\ \right] \\ & = Dynamic\ Stiffness = [H\ ]^{-1} \end{aligned} \tag{4}$$

$$[Synchronous\ Dynamic\ Stiffness] = \left[\underline{H}\right]^{-1}$$

and by comparison between equations (4 y(1, the synchronous dynamic stiffness is identified in this last equation (4.

Therefore, the vibration of a machine will depend on changes in the disturbance force or the characteristics of the dynamic stiffness of the structure, or both. A modification of the rotor balance is identified by an alteration of disturbing force, while a crack in the shaft/rotor or in the machine bench, a loss of tightening in the machine's supports, or an impoverishment in lubrication, is corresponding to a modification of its dynamic stiffness. In this way, one can give the paradox that a decrease in the vibration response does not respond to a lower disruptive force, but to an increase in its stiffness, and hence the importance of knowing its values.

III. Unbalance

Unbalance is the most frequent breakdown in rotating systems. During the operation, the axis of rotation does not coincide with the rotor mass centreline. The rotor unbalance generates an inertial centrifugal force that rotates at the rotation frequency of the rotor. The mathematical model of an isotropic unbalanced at its first lateral mode is as follows:

$$M\ddot{z}_{\text{inertia force}} + D(1-\lambda)\dot{z}_{\text{damping force}} + Kz_{\text{stiffness}} - jK_r\{\varphi(\Omega)\}\, z_{\text{tangential stiffness}} = mr_u\ \Omega^2 e^{j(\Omega t+\delta)}{}_{\text{centrifugal force}} \quad (5)$$

The equation (5 represents the balance of forces stand-in the rotor, as well as the tangential forced depending on the speed of rotation $[K_r\{\varphi(\Omega)\}z]$. The component (1-λ) corresponds to the rotor damping reduction due to the fluid tangential forces (for supports, seals or bearings with pressurized fluid lubrication). The left side of the equation (5 identifies with the rotor restraints, i.e. its dynamic stiffness and the right side, the inertia unbalance force. The rotor response is observed by one lateral displacement will represent a sinusoidal waveform, with frequency equal to the rotational speed Ω, amplitude "A" and phase lag "α". The solution of equation (5 is:

$$z = Ae^{j(\Omega t+\alpha)},\ wich\ replaced\ in\ equation(5, \text{ it turns out:}$$

$$[K - M\Omega^2] + jD(1-\lambda)\Omega - jK_r]_{\text{dynamic stiffness}} \cdot Ae^{j\alpha}{}_{\text{response}} = mr_u\Omega^2 e^{j}{}_{\text{unbalance force}} \quad (6)$$

The rotor response depends of its dynamics stiffness and unbalance, so any change in the rotor response may result from a change either in unbalance or in the restraining rotor dynamic (e.g. a crack implies a decrease in stiffness, while a rubbing axle/support increases).

The amplitude and phase lag, can be determine from equation (5:

$$A = \frac{mr_u\Omega^2}{\sqrt{(K - M\Omega^2)^2 + [D\ (1-\lambda)\Omega - K_r]^2}} \quad ; \quad \alpha = +arc.tg.\ \frac{K_r - D(1-\lambda)\Omega}{K - M\Omega^2} \quad (7)$$

This equation (7 show which when the speed rotative $= \sqrt{\frac{K}{M}}$, the response amplitude reach a resonance peak, because the denominator of this equation only be controlled by the small damping term: $[D\ (1-\lambda)\Omega - Kr]$, and the phase lag "α" = δ (angular position of unbalance) + 90º.

Bode and polar plots, during rotor start-up or shutdown, rotor 1Ω filtered response measure by a displacement transducer, identify the first balance resonance frequency and the unbalance location. Figure 1: (heavy spot = angular position of the unbalance vector, at a specific lateral location on the shaft); (high spot = angular location on the shaft under the vibration probe at that point in time, when the shaft makes its closest approach to that probe).

It should be noted that the response to unbalance is identical in all transverse directions, as this phenomenon is inherent in the rotor and accompanies it in its rotation.

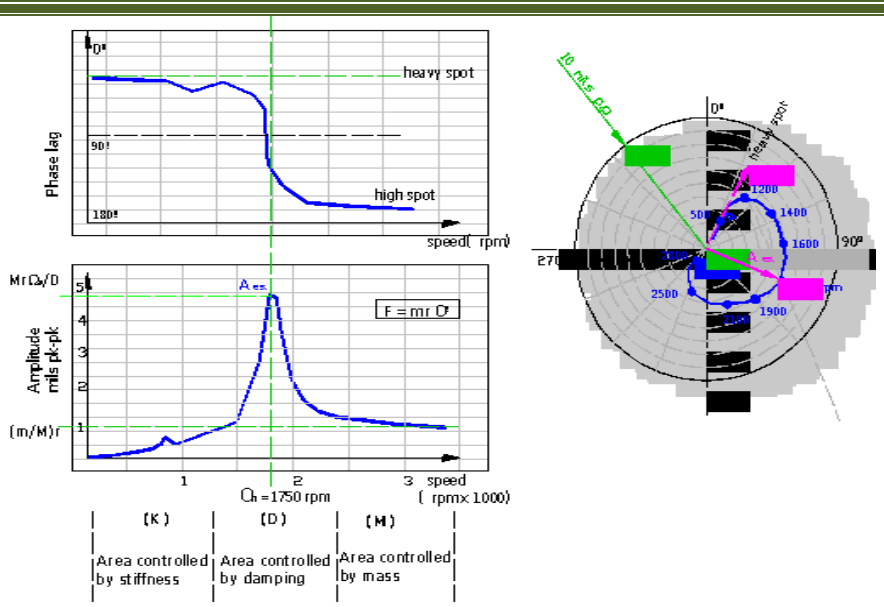

Figure 1. Bode and polar plots

From equation (5, which represents the mathematical model of an unbalance, it is also useful for identifying the components of dynamic stiffness, using the method by the known synchronous unbalance disturbance [4], described already in paragraph 2:

$$Direct\ Dynamic\ Stiffness\colon\ K_D = K - M\Omega^2 = \frac{[mr_u\Omega^2 cos(\theta - \alpha]}{A} \tag{8}$$

$$Quadrature\ Dynamic\ Stiffness\colon\ K_Q = D(1-)\Omega - K_r = \frac{[mr_u\Omega^2 sin(\theta - \alpha]}{A} \tag{9}$$

These dynamic stiffness components can be represented versus rotation speed to identify modal stiffness, mass and system damping, Figure 2.

The method of a synchronous external force is generally used for rotor balancing, and the influence vectors used correspond to the inverse of the dynamic stiffness matrix, which are often dismissed, when in fact they are very useful to observe future changes in this stiffness, which can diagnose events such as shaft cracks, rubs or others, equations (1 to (4.

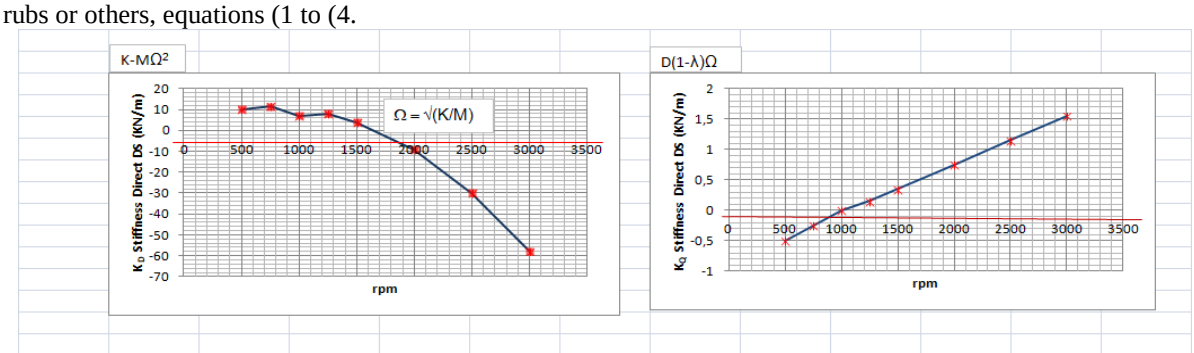

Figure 2. Dynamic Stiffness

IV. Rubbing shaft to stator

The rubbing appears on the machine when a contact between the rotor and a static element arises (mechanical seals, labyrinth closures, diaphragms, retainers, etc.). Always occurs as a secondary effect of a primary malfunction, its can even start with a strong unbalance, a very pronounced curvature, thermal expansions, fluid induced vibrations or incorrect alignments.

A rub of a certain magnitude destroys the machine quickly and, therefore it is very important to detect it in its initiation as partial rubbing. Once the full annular rub is reached on the entire rotor/stator contour, the damage to the machine is already very severe and should be stopped immediately.

IV.1 Partial rubbing

Partial rubbing forces are added to the mathematical expression of the lateral movement of a simple rotor model equation (5, according Figure 3 and Figure 4: [5]

$$M\ddot{z} + D\dot{z} + Kz + \underbrace{F(\Omega_r t)[K_o|z| + N(1+j\mu)]e^{j\beta}}_{influence\ \ of\ \ partial\ \ rubbing} = mr_u\,\Omega^2 e^{(j\omega t+\delta)} \qquad (10)$$

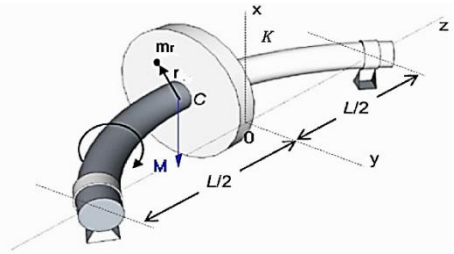

Figure 3. Rotor deflection

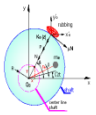

Figure 4. Cross section-shaft

Assuming that the shaft contacts the obstacle a fraction of the rotation, the function $F(\Omega_r t)$ can be modelled by a periodic function, depending on time intervals, in which Ωt1 represents the time of the first contact and 2π the end of the contact, Figure 5:

$$F(\Omega t) = 1 - \frac{\left\{\frac{\Omega t_1}{2} - \sum_{i=1}^{n} \frac{2}{i}\, sin\, sin\, (i\frac{\Omega t_1}{2}\, cos\left[i\Omega\left(t - \frac{\frac{t_1}{2}}{2}\right)\right]\right\}}{\pi} \qquad (11)$$

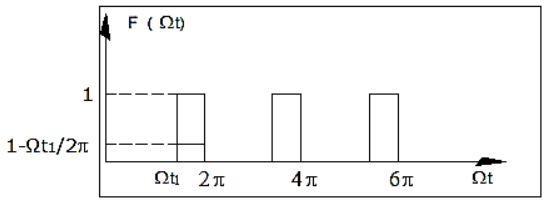

Figure 5. Periodical function

The solution of the rotor model for action of the average value of the radial force P = N(1-$\Omega t_1/2\pi$), is as follows: [6]:

$$z(t) = \underbrace{\left(\dot{z}_o + \xi\,\frac{P(1+j\mu)}{K}\Omega_n e^{j\beta} - j\Omega\, R\, e^{j\beta}\right)\frac{1}{\Omega_n} e^{-\xi\Omega_n t}\, sen\, \Omega_n t}_{dampened\ \ free\ \ vibrations}$$

$$+ \underbrace{\frac{P(1+j\beta)}{K} e^{j\beta}\left(e^{-\xi\Omega_n t}\, cos.\, \omega_n t - 1\right)}_{action\ \ of\ \ the\ \ radial\ \ force\ \ of\ \ impact\ "P"} \qquad (12)$$

$$+ \underbrace{R\, e^{j(\Omega t+\beta)}}_{forced\ \ vibration\ \ of\ \ unbalance\ \ caused\ \ by\ \ the\ \ rebound\ \ of\ \ the\ \ collision}$$

This solution is valid during the time interval [0, t_1], where $\Omega_n = \sqrt{\frac{K(1-\xi^2)}{M}}$ is the rotor natural frequency and $\xi = \frac{D}{2\sqrt{KM}}$ is the damping factor. For very light partial rubs, at rotative speeds exceeding double value of the first balance resonance speed and these vibrations superposed on unbalance forced vibrations (1Ω) result in fractional sub synchronous vibrations: ½, 1/3, etc., situation that can be observed in the Figure 6.

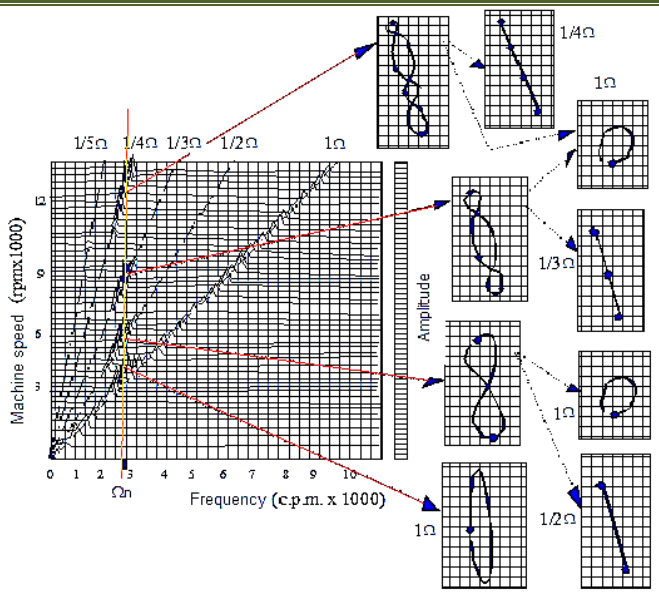

Figure 6. Spectrum cascade and corresponding orbits

IV.2 Full annular rub.

During the rotor rubbing to stator or rotor to seal, full annular rub occurs dynamic effects as friction, modification of the stiffness and the effect of radial clearance which are taken in the mathematical model of the rotor. The system becomes mathematical continuous with variable stiffness. The modal stiffness K is now split in three sections, Figure 7, K=$K_3 + \frac{K_1 K_2}{K_1+K_2}$, and the mathematical model of the rotor maintaining contact with the seal is: [7]

$$\begin{aligned} M\ddot{z} + D(1-\lambda)\dot{z} + K_2(z - z_2) + K_3 z &= m r_u \Omega^2 e^{j\Omega t} \\ K_2 z - z_2[K_1 + K_2 + (\psi_1 - \psi_2)(z_1)] &= 0 \\ z_1(z_1) + K_1 z_2 + K_2(z_2 - z) &= 0 \end{aligned} \tag{13}$$

where, □ (z1) is a function correspondingly to seal dynamics characteristics:

$$(z_1) = \frac{[M_s \ddot{z}_1 + D_s \dot{z}_1 + K_s z_1(1+j)]}{z_1}[\ {}_1(z_1) + j\ {}_2(z_1)] \tag{14}$$

Ms, Ks, Ds, η are the seal mass, stiffness, damping and material loss factor and ψ_1, ψ_2 are nonlinear functions of the displacement z_2:

$$\psi_1 = 1 - \frac{R-r}{|z_2|^2(1+\mu^2)}[(R-r)\mu^2 \pm] ; \quad \psi_2 = \frac{(R-r)\mu}{|z_2|^2(1+\mu^2)}[(R-r) \pm] \tag{15}$$

being, $\Delta = \sqrt{|z_2|^2(1+\ \ ^2) - \ \ ^2(R-r)^2}$; $= \frac{^*-}{1+\ ^*}$; $=\ \ {}_2(z_1)/[\ {}_1(z_1)]$

(R – r) is the shaft-seal clearance, and y μ* is dry friction coefficient.

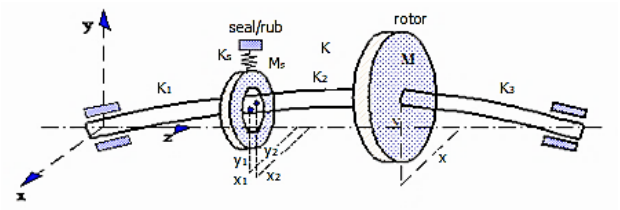

Figure 7. Model of the rotor

When the full annular rubbing takes place throughout the rotation, $z_1 = z_2$, (R-r) = 0, $\psi_1 = 1, \psi_2 = 0$, the system becomes linear and the forced solution of the modified resultant of this values in the equations (13 has the following form: [7]

$$z(t) = Be^{j(\Omega t+\beta)} \; ; \qquad z_1(t) = z_2(t) = B_1 e^{j(\Omega t+\beta_1)} = B_2 e^{j(t+\beta_2)} \tag{16}$$

and the amplitudes and phase lag are [8]:

$$B = \frac{mr_u\Omega^2}{\sqrt{h_1^2 + D^2\Omega^2 + K_2^2\,(K_2^2 - 2h_1h_2 + 2D\Omega h_3)/\,(h_2^2 + h_3^2)}}$$

$$B_1 = B_2 = \frac{mr_u\Omega^2 K_2}{\sqrt{(h_1^2 + D^2\Omega^2)\,(h_2^2 + h_3^2) + K_2^2\,(K_2^2 - 2h_1h_2 + 2D\Omega h_3)}}$$

$$\beta_1 = \beta_2 = arctang\frac{D\Omega h_2 + h_1h_3}{K_2^2 + D\Omega h_3 - h_1h_2} \quad ; \quad \beta = \beta_1 + arctg\,(\frac{h_3}{h_2})$$

where: $h_1 = (K_2 + K_3) - M\,\Omega^2$, $h_2 = (K_1 + K_2 + K_s) - M\,\Omega^2$, $h_3 = D_s\,\Omega + D_s\eta$.

In addition, for very small damping values, such as a solid contact between shaft and mechanical seal: $D = D_s = \eta = 0$, the vibration amplitudes indicated in the above equations become:

$$B = \frac{mr_u\,\Omega^2 h_2}{F(\Omega)} \; ; \; B_1 = \frac{mr_u\,\Omega^2 K_2}{F(\Omega)} \tag{17}$$

$$where:\ F(\Omega) frequency function = |(K_1 + K_2)(K - M\Omega) + (K_S - M_S\Omega^2)(K_2 + K_3 - M\Omega^2)| \tag{18}$$

From the equation $F(\Omega) = 0$, the natural frequency of the rotor-seal system is obtained, where for highs values of the seal natural frequency $\left[\sqrt{\frac{K_s}{M_s}}\right]$ are approximately equal to the following expression:

$$\Omega_2^{n(cou)}(with\ rub)\sqrt{(K_1 + K_2 + K_s)/M_s} \tag{19}$$

which in comparison to the uncoupled shaft/seal system: $\Omega_2^{n(un)}(without\ rub) = (-1)^i\sqrt{K/M}$, it is noted an increase of the natural frequencies: $\left\{\omega_2^{n\,(un)} < \omega_2^{n\,(cou)}\right\}$. The "mechanical seal", therefore, behaves as "a new bearing" added, and increases the stiffness of the system and, consequently, the value of the natural resonance frequency of that coupled system, as shown in Figure 8 and Figure 9. When the rotational speed reaches a limit, the shaft loses contact with seal and its response decreasing, the phase angle is nearly constant, then sharply drops down when the shaft/seal contact is lost.

The coupled shaft/seal system response depends powerfully on the clearance (R-r=1 to 0,25 mm), Figure 9. The actual maximum amplitude depends on the shaft/seal radial clearance. The rotor response (Figure 8) depends on whether the rotational speed is increasing or decreasing. Since model of equation (13 includes rub generated non-linear term, the rotor response, besides the fundamental components (1X response), contain a spectrum of higher harmonics (2X, 3X ...), Figure 10. [9]

It is studied a simple mathematical model of the rotor full annular rub. When the rotor and seal are in contact, there are two major regimes of the rotor motion:

i.-) Forced synchronous precession due to unbalance, and

ii.-) self-excited circular backward precessions with frequencies corresponding to the natural frequencies of the coupled shaft/seal system. The analysis of the all effects were not includes here.

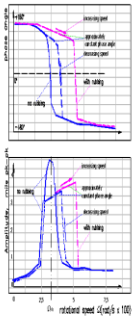

Figure 8. Bodé of the synchronous of the annular shaft/ seal rub.

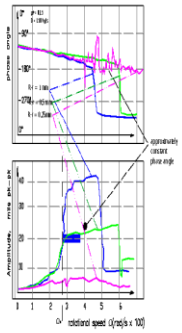

Figure 9. Bodé of the synchronous of the rotor with 1, 0,5 and 0,25 mm radial clearance seal.

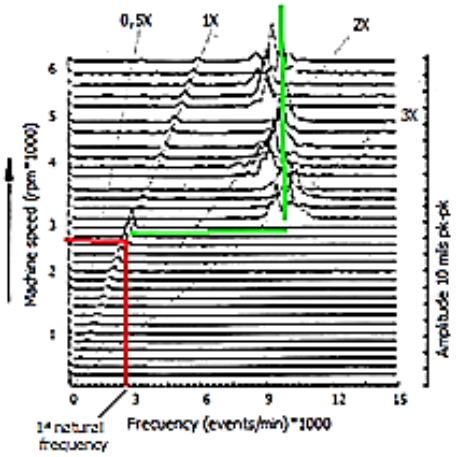

Figure 10. Cascade spectrum. Full annular rub.

V. Misalignment

The misalignment between power transmission shaft supports and couplings is one of the most common latent defects of machines and their installation. They may not even be important at first, but they are underlying assembly and over time they can have devastating effects; hence the importance of their study and surveillance on machines.

A misalignment between the supports of a rotor, for example due to a seat or bearing wear, produces an external radial load that acts only on the misaligned plane. For shaft monitoring, would be installed two induction transducers at 90º (H and V) plus the phase reference transducer. The movement of a shaft with this phenomenon is represented by [10]:

$$M\ddot{x} + D_x(1-\lambda_x)\dot{x} + K_x x - K_{rx}(\Omega)y = \dot{m}r\Omega^2 \cos\cos(\Omega t + \delta) + P\cos \quad (20)$$

$$M\ddot{y} + D_y(1-\lambda_y)\dot{y} + K_y y - K_{ry}(\Omega)x + (K_n y + \dot{\cdots})y = mr\Omega^2 \sin\sin(\Omega t + \delta) + P\sin \quad (21)$$

where P, in this case, is the preload applied to the shaft in the radial direction, with the angle γ regarding the axes X e Y, δ is the unbalance angular location and K_n is a generalized nonlinear stiffness coefficient.

The radial force that causes the misalignment is not internal, but external. It is not a force that rotates with the shaft, but remains static in the direction that occurs, such as the forces of gravity or a load of hydraulic pressure, that distorts the circle orbit that describes the centre of the shaft to form orbit models. The radial force increases and thus the restriction to shaft movement. The orbit ceases to be circular or somewhat elliptical to take much compressed forms of "banana", even "eight" in the direction of that radial load, Figure 11.

As the orbit changes from an elliptical shape to "banana" shape, it´s also a indication that higher frequency components are present.

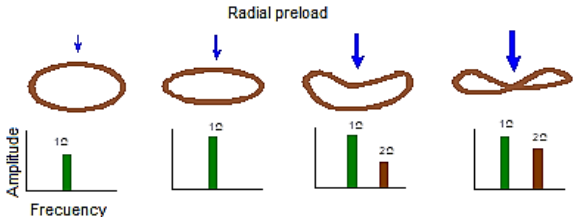

Figure 11. Misalignment, frequency spectre and orbits

Another fact that occurs due to misalignment is that the situation of the centre of the shaft in the bearings of both supports will appear in contrasting quadrants, as indicated by the Figure 12 in positions "1" and "2", which is where the shaft will end up performing the orbit of motion. This situation does not identify in itself the anomaly of misalignment, but because of the simple control, thanks to the proposed installation of two induction transducers at 90º, it is very useful to avoid catastrophic breakdowns.

Axial measurements can also indicate a problem of misalignment in the machine, as it causes the "N" axial force and, consequently, a vibration in the axial direction will be detected.

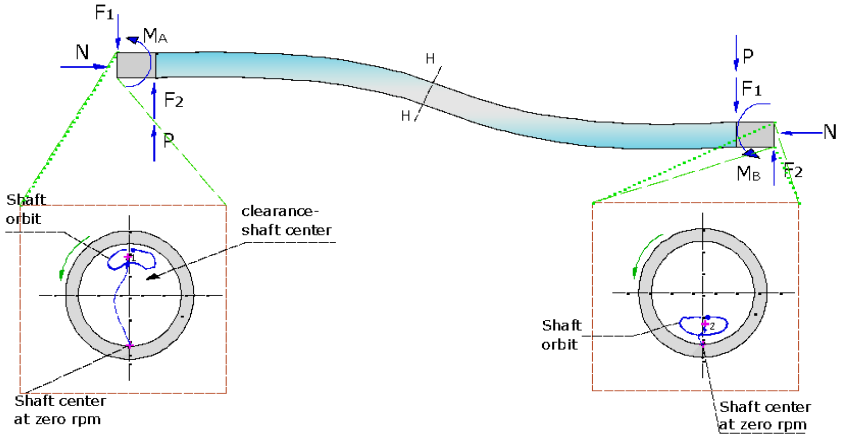

Figure 12. Misalignment, centreline positions

Identified the misalignment plane as y-y plane, the equations(20)and((21), which is the most common, and their solution is [11]:

$$x(t) = A_x \, cos \, cos \, (\Omega t + \alpha_x) \tag{22}$$

$$y(t) = A_0 + A_1(\Omega t + \alpha_1) + A_2(2\Omega t + \alpha_2) \tag{23}$$

in which the 2X response is already observed in the assumed vertical plane of the misalignment amplitude A_2, frequency 2Ω, and phase angle α_2, with A_o being the static to rotor displacement stopped as a result of the misalignment in that plane.

The Figure 13 shows the cascading spectrum of the response in the misalignment plane, in which the following particularities can be underlined:

• Maximum amplitude in the 1X response, coinciding with the resonance frequency, and overall increase of this response by the increased mass unbalance that results in the eccentricity of the shaft with the misalignment. Other minor increments occur in multiples of that speed.

• Maximum amplitude of the 2X response at the rotation speed coincident with the resonance frequency and half its value (0.5 res.) Generally, greater amplitude of the 1X response than the 2X, as the mass unbalance effect produces the eccentricity of the misalignment shaft than the radial load that produces externally that misalignment.

• Concurrency of the amplitude increments of 1X and 2X responses.

• 2X vibration response only on the misaligned plane and not on the other perpendicular. Asymmetry, therefore, in the response of the two transducers located at 90º (this situation would not be perceived with the typical installation of an accelerometer on a transverse plane).

• Radial vibration increases with rotation speed.

• The orbit describing the centre of the shaft is modified. Where only 1X response exists, the orbit is almost circular (schema a) in Figure 13), whereas when the 2X response appears and as the magnitude of the latter increases. The orbits restrict their movement in the line-up plane in which it is produced the force "P" and flattened orbits are presented, in the form of "bananas" or "eight", as indicated in diagrams (b) and (c) in Figure 13.

At slow axis rotation speeds, at values equal to half the resonance frequency (0.5 res.) there are already amplitude increases of the 1X response, and not 2X, because already at those low-value speeds, due to the large mass unbalance that is produced by the eccentricity of the misaligned shaft. A vibration of the unbalance without 2X response already appears. This phenomenon is unique to the misalignment and does not appear in other anomalies that have somewhat similar responses such as transverse cracks or shaft curvatures, since although they have both 1X and 2X responses, in these cases, the added unbalance does not result so significant to be displayed at small rotational speeds ($F = mr\Omega^2$).

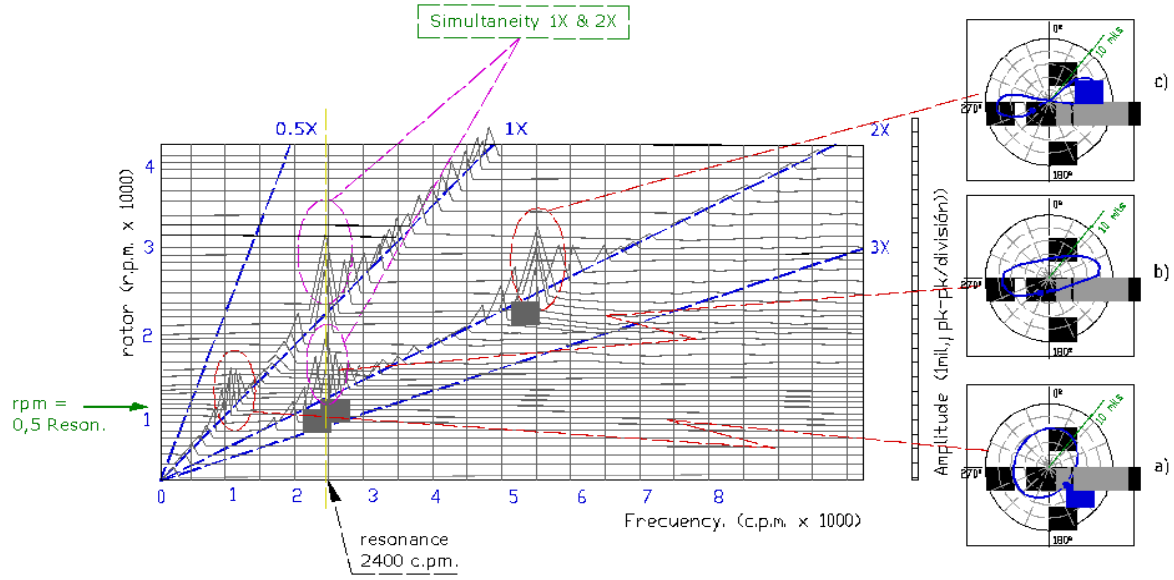

Figure 13. Misalignment. Cascade spectrum.

It is assumed also that there will be no coupling between the answer on the "x" and "y" axis, so the model of equation (22 corresponds exclusively to a rotor with the corresponding residual unbalance without any other anomaly on that plane, and its response on the axis "x", will therefore be:

$$A_x = \frac{mr\Omega^2}{\sqrt{(K - M\Omega^2)^2 + [D(1-\lambda)\Omega]^2}} \quad (24)$$

$$\alpha_x = \delta + arctang\ \frac{D(1-\lambda)\Omega}{K - M\Omega^2} \quad (25)$$

For the misalignment plane y-y, equation (23 is replaced in equation (21, and it's obtained the five parameters of response unknown of this plane: the static displacement A_o, the amplitude and phase A_1 and α_1, of the synchronous response (1X), and the amplitude and phase A_2 and α_2 of the second harmonic (2X) [11]:

$$A_0 = -\frac{K}{2K_n} + \sqrt{\left[\frac{K}{2K_n}\right]^2 + \frac{P}{K_n} - \frac{A_{1+}^2 A_2^2}{2}} \quad (26)$$

$$A_1 = \frac{mr\Omega^2}{\sqrt{(K - M\Omega^2 + 2K_n A_0 + K_n A_2 cos.\varepsilon)^2 + (D\Omega + K_n A_2 sen.\varepsilon)^2}} \quad (27)$$

$$A_2 = \frac{K_n A_1^2}{2\sqrt{(K - M\Omega^2 + 2K_n A_0)^2 + (2D\Omega)^2}} \tag{28}$$

$$\alpha_1 = \delta + arctg.\frac{D\Omega + K_n A_2 sen\ \varepsilon}{M\Omega^2 - K - 2K_n A_0 - K_n A_2\ cos\ cos\ \varepsilon} \tag{29}$$

$$\alpha_2 = 2\alpha_1 + \varepsilon - 90º \tag{30}$$

$$siendo:\ \varepsilon = arc\ tg.\frac{2D\Omega}{4M\Omega^2 - K - 2K_n A_0}$$

For a high speed constantly operating machine, the number of the stress reversal cycles may quickly reach the fatigue limit.

VI. Fluid Induced Instability

Dynamic phenomena induced by interaction between the rotor and stator or seal fluid motion create severe rotor vibrations and that its correlate to self-excited vibration known as "oil whirl" and "oil whip". This interaction becomes significant if the clearances between rotating and stationary parts are small, and the rotors operate at low eccentricity within these clearances, Figure 15.

The simple mathematical model of the rotor in a system like that of the Figure 14, supported in one antifriction and one rigid bearing fluid lubricated bearing or seal, where the unbalanced forced is assumed equal to zero, to investigate the ability of the purely rotational motion of the shaft, is:

$$Rotor: \quad M_1\ddot{z}_1 + D_S(1-\lambda)\dot{z}_1 + (K_1 + K_2)z_1 - K_2 z_2 = 0 \tag{31}$$

$$Seal: \quad M_2\ddot{z}_2 + M_f(\ddot{z}_2 - 2j\lambda\Omega\dot{z}_2 - \lambda^2\Omega^2 z_2) + [D + \ _2(|z_2|)]\,(\dot{z}_2 - j\lambda\Omega z_2) + [\,K_{eo} + \ _1(|z_2|)]z_2 + K_2(z_2 - z_1) = 0 \tag{32}$$

where K_o, D and M_f are fluid stiffness, damping and inertia coefficients. Ψ_1 and Ψ_2 are fluid nonlinear functions of journal radial displacement z_r and D_s is the generalized external viscous damping coefficient.

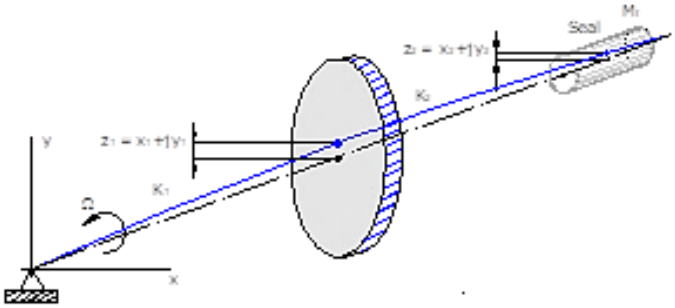

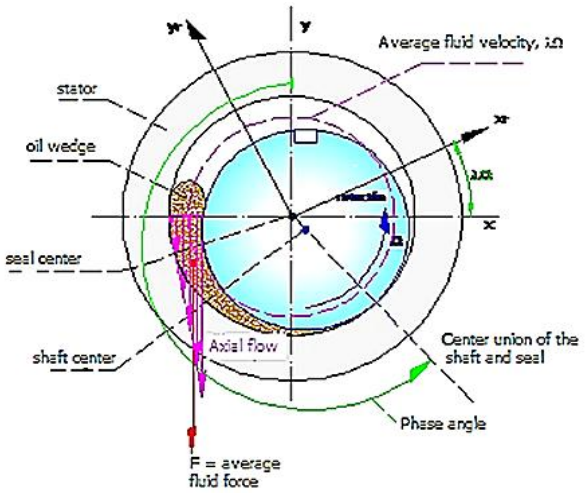

Figure 15. Seal model. Fluid force is rotating with angular velocity λΩ

In absence of unbalance, and for the investigate the ability of the stability analysis, the nonlinear terms in the equation (32 are neglected as they are small and of second order. Therefore, theses equations (31 and (32 have a particular solution that describe self-excited vibration by fluid instability: [12]

$$z_1 = E_1 e^{st} \quad ; \; z_2 = E_2 e^{st} \tag{33}$$

s = the eigenvalue of the rotor/seal system.
E_1, E_2 = constants of integration
that leads to the characteristic equation:

$$\begin{aligned}\left[M_2 s^2 + M_f (s - \lambda\Omega)^2 + D(s - j\lambda\Omega) + K_0\right](K_1 + K_2 + D_s s + M_1 s^2) \\ + K_2(K_1 + D_s s + M_1 s^2) = 0\end{aligned} \tag{34}$$

The approximate values of three eigenvalue of equation (34 are as follows:

$$s_1 \approx \left[\frac{Ke_0}{D}\right] - \left[\frac{K_2(K_1 - M_1\lambda^2\Omega^2)}{D(K_1 + K_2 - M_1\lambda^2\Omega^2)}\right] + j\,\lambda\Omega \tag{35}$$

$$s_{2,3} \approx \frac{-D_s}{2M_1 \pm j\sqrt{R_1 - jR_2}} = \frac{-D_s}{2M_1 \pm \frac{\left[-\sqrt{-R_1 + \sqrt{R_1^2 + R_2^2}} + j\sqrt{R_1 + \sqrt{R_1^2 + R_2^2}}\right]}{\sqrt{2}}} \tag{36}$$

$$para\ \lambda\Omega < \sqrt{\frac{(K_1+K_2)}{M_1}} = rotor\ natural\ frecuency, and\ where:$$

$$R_1 = \left[\frac{(K_1 + K_2)}{M_1}\right] - K_2^2\left[K_0 + K_2 - \frac{M_2(K_1 + K_2)}{M_1} - M_f\left(\pm\sqrt{\frac{(K_1 + K_2)}{M_1}}\right)^2 - \lambda\Omega\right]/R_3$$

$$R_2 = -K_2^2 D\left(\pm\sqrt{(K_1 + K_2)/M_1}\right) - \lambda\Omega/R_3$$

$$R_3 = \left\{\left[K_{e0} + K_2 - \frac{M_2(K_1 + K_2)}{M_1} - M_f\left(\pm\sqrt{(K_1 + K_2)/M_1} - \lambda\Omega\right)^2\right]^2 + D^2\left(\pm\sqrt{(K_1 + K_2)/M_1} - \lambda\Omega\right)^2\right\}M_1$$

The imaginary parts of the eigenvalue, equations (35 and (36 represent the natural frequencies of self-excited vibrations "oil whirl" and "oil whip". In the first natural frequency (s_1) is close to λΩ, equation (35, when the rotation velocity Ω has a low value, and that it tends to the constant value, when Ω increases, corresponding to the rotor natural frequency $\sqrt{(K_1 + K_2)/M_1}$[12]. The second natural frequency ($s_{2,3}$) is close to the rotor natural frequency $\sqrt{(K_1 + K_2)/M_1}$, Figure 16 and Figure 17.

The real part of the eigenvalue, equation (35, predicts the threshold of stability (Ω_{ST}) which is when the phenomenon of "oil whirl" begins, Figure 17.

For rotation speed Ω:

$$\Omega_{ST} = \frac{1}{\lambda}\sqrt{\frac{K_1}{M_1} + \frac{K_2\left(K_{e0} - \frac{M_2 K_1}{M_1}\right)}{M_1\left[K_2 + \left(K_{e0} - \frac{M_2 K_1}{M_1}\right)\right]}} \tag{37}$$

$= real\ part\ of\ the\ eigenvalue, equation\ REF\ \_Ref25263006\ \h\ *\ MERGEFORMAT\ \ * MERGEFORMAT$ (35

$$It\ is\ assumed\ that\ M_2 \to 0\ compared\ to\ M_1$$

In this range the rotor rotational motion is stable, and for $\Omega > \Omega_{ST}$ the rotational motion become unstable. The first term in equation (37, K_1/M_1 is dominant. In the second term which contains two stiffness: $K_2 + \left(K_{e0} - \frac{M_2 K_1}{M_1}\right)$, K_{e0} and the mass M_2 are small , therefore the equation (37 by defining the rotor/seal system stability threshold as:

$$\Omega_{ST} \approx \left(\frac{1}{}\right)\sqrt{\frac{K_1}{M_1}} \tag{38}$$

An increase of the stiffness K_1 *cause* a significant increase of the threshold of stability.

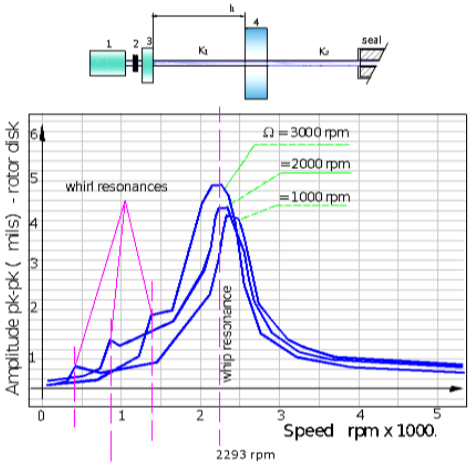

Figure 16. Bode diagram, oil whirl and oil whip

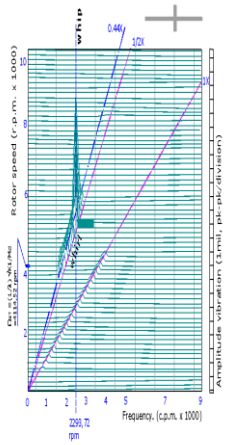

Figure 17. Cascade spectrum, oil whirl and oil whip and stability threshold.

VII. Threshold Stability

The general expressions of the fluid dynamic apply to the rotor are:

$$\begin{bmatrix} F_x & F_y \end{bmatrix} = \begin{bmatrix} K_{xx} & K_{xy} \\ -K_{yx} & K_{yy} \end{bmatrix}\begin{bmatrix} x & y \end{bmatrix} + \begin{bmatrix} D_{xx} & D_{xy} \\ -D_{yx} & D_{yy} \end{bmatrix}\begin{bmatrix} \dot{x} & \dot{y} \end{bmatrix} + \begin{bmatrix} M_x & 0 \\ 0 & M_y \end{bmatrix}\begin{bmatrix} \ddot{x} & \ddot{y} \end{bmatrix} \tag{39}$$

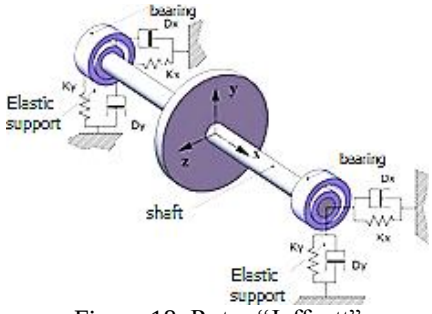

Figure 18. Rotor "Jeffcott"

Dynamic stiffness of rotor is studied by applying a perturbation force of sinusoidal nature to the rotor at the frequency "ω". Dividing the perturbation force vectors by the corresponding response vectors yields the dynamic stiffness vectors and the force balance relationship for a concentrically rotating shaft at the seal or bearing are:

$$\underline{F}_{pert\,-z} = \left[K_B - (\omega -)^2 M_f + jD(\omega -) + K - M\omega^2 + jD_s\omega\right]\underline{z} \tag{40}$$

From equation (40 system dynamics components are obtained:

$$Direct\ stiffness\colon\ K_D = \left(\frac{F_{pert\,-z}}{|z|}\right) * cos\ cos\ \alpha = K_B - (\omega -)^2 M_{fl}{}_{\omega\ fluid\ parameters} + K - M\omega^2{}_{\omega\ rotor} \tag{41}$$

$$Quadrature\ stiffness\colon\ K_Q = -\left(\frac{F_{pert\,-z}}{|z|}\right) * sin\ sin\ \alpha = D(\omega -)_{\omega\ fluid} + D_s\omega_{\omega\ rotor} \tag{42}$$

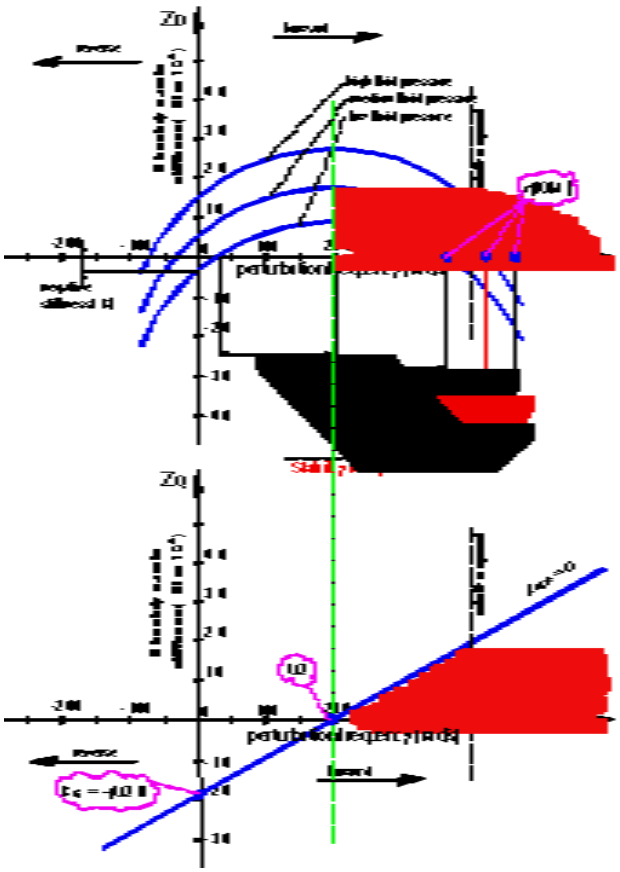

Figure 19. Dynamic stiffness versus frequency for several values of fluid pressure.

The Direct Dynamic Stiffness versus frequency of perturbation force "ω" is a parabola shifted from the axis origin due to fluid inertia. The effect of higher pressure causes an increase of K_B. For ω=0, the Direct Dynamic Stiffness $\{K_D = K \_ \lambda^2\Omega^2 M_{Fl} + K_B\}$ and for small values of $(K+K_B)$ this Direct Stiffness can be negative, Figure 19.

The Quadrature Dynamic Stiffness versus frequency is a straight line, but displaced from the coordinate origin for the same reason, which cross the vertical axis at its negative side, and its value is the seal/bearing cross stiffness $\{-j\lambda\Omega D\}$, Figure 19. The slope of the straight line is "D".

In this case, the actual component of dynamic stiffness, for the same mechanical seal or bearing, depends on the pressure of the fluid, so that, at higher pressure more stiffness, as shown in Figure 19, while the imaginary component is independent of the fluid pressurization [13]. The stability margin is shown, in this Figure 19 as the common area between the two graphical representations of Z_D and Z_Q, which is where they have positive values, and therefore a higher value dynamic stiffness, thus providing vibration amplitude responses less:

$$Response\ Amplitide = \frac{Pertubaation\ force}{Dynamic\ stiffness}$$

The fluid pressure in the seal/bearing rises with the velocity square and the stiffness of the pressurized fluid is increased linearly with that pressure (K_B), so the actual component of dynamic stiffness is also increased with the velocity square. Once the fluid pressure is controllable, dynamic stiffness is also controllable, and as can be seen in Figure 19. At higher fluid pressures are achieved wider stability zones for the rotors, so that the value of the fluid pressure will already indicate the state of the dynamic stiffness and attenuation of the lubrication fluid film, as well as being able to achieve better stability margins.

VIII. Conclusions

The analysis of collected database from machinery monitoring systems, and from laboratory simulations allows for correlations of particular breakdowns between the machine design and operational

conditions. The accumulated practical knowledge supported by simple mathematical modelling must be absorbed and implemented by machinery manufacturers.

At the present time health monitoring of machines becomes gradually automated. The use of computer instruments and computer system to collect, record and process the data has become a routine. Expert systems are natural extensions of this trend.

Expert systems are cost effective only when applied to specific classes of machines which operate in large numbers. High complexity and resulting high development costs of the expert systems are representative only if they can be amortized over a large number of sales, for a wide variety of rotating machines operating in a large multitude of process is still imperfect actually. A second major problem is that the responses and recommendations are stated only as probabilities, thus expert human judgements are still required to asses these probabilities.

A true expert system must be capable of totally replacing a human expert in the machine operation control, diagnosis and corrective actions. Human experts, with their intuitive abilities, will always be required to provide solutions for most occasionally come upon problems, or all malfunctions which exhibit any asymptomatically characteristics.

Expert systems must always be considered as useful tool to assist in the machinery diagnosis, not as main goals.

Nomenclature:

M, D and K = mass, damping and spring coefficient of the rotor.
x, y, horizontal and vertical deflections of the rotor disc.
m, r_e and Ω, are the mass of the imbalance, the radial and angular position of the imbalance.
Ω = rotation speed.
K_r = tangential stiffness versus rotation speed Ω.
λ = average circumferential component of fluid flow ratio to rotative speed in the seal.
1-λ = damping reduction effect due to fluid tangential forces
K_o - additional stiffness due to the new support that involves rubbing.
N = radial force due to impact/bounce.
P (rubbing) = value of the periodic radial force of the rub: $P = N(1 - \Omega t/2\pi)$
Ω_r = frequency of rotational precession movement in reverse on impact.
$F(\Omega_r t)$ = function indicative of the effects of periodic forces of friction on rotation.
$K_0|z|$ N and μN = effects of the change in rigidity, impact and friction due to the obstacle, (μ =friction coefficient).
R, β = radial and angular position of the obstacle/collision.
ξ = damping factor.
Ω_n = natural frequency.
$z'_0 = x`_0 + y`_0$ = initial velocity after impact.
$_1(|z_2|), and \quad _2(|z_2|)$ are non linear functions of the radial displacement z_2
K_n = nonlinear stiffness coefficient that appears as a result of this displacement of the rotor by the misalignment of the shaft.
K_o, D and M_f are fluid stiffness, damping and inertia coefficients.
M_1, M_2 rotor and journal masses.
F_x, F_y perturbation force of sinusoidal according to X and Y axes,
K_x, K_y stiffness, X and Y axes.
K_{xy} K_{yx} interference stiffness from one direction over the other.
M_x, M_y mass according both axes (on the Y axis adds the influence of gravity)
ω, vibration response
$\underline{F}_{pert\ -z}$ is the sinusoidal circular disturbance force.
$\underline{z} = x + jy$ is rotor lateral response vector at frequency ω.
K_B is the sum of the hydrodynamic plus hydrostatic bearing or seal fluid film stiffness.
α is angle between perturbation force and rotor response.

Bibliografía

[1]. Z. Peng, «Expert system development for vibration analysis in machine condition monitoring,» *ScienceDirect. Elsevier Ltd. https://www.researchgate.net/publication/222432519*, nº DOI: 10.1016/j.eswa.2006.09.029, 2016.

[2]. International Organization for Standardization (ISO), «"Measurement and Evaluation of Mechanical Vibration of Non-Reciprocating Machines as Measured on Rotating Shafts", document DP 7919.,» ISO, Geneva, Switzerland., 1996 (last reviewed: 2012).

[3]. A. Curami y A. Vania, «Model idetification in computer-controlled monitoring of rotor machinery,» de *Fourth International Conference on Rotor Dynamics*, Chicago, Illinois., 1994.

[4]. B. Fraga, «Study of the stability margin and its connection with the dynamic stiffness applied to a tidal turbine. Id. 201901002,» *International Journal of Latest Engineering Research and Applications (IJLERA)*, vol. 04, nº 01, p. 11, January, 2019.

[5]. Hayashida, Franklin y Muszynska., «Rotor-to-stator partial rubbing and its effects on rotor dynamic response. pp. 345-362.,» de *The Sixth Workshop on Rotordynamic Instability Problems in High Performance Turbomachinery*, College Station, Texas. Nasa., 1990.

[6]. J. Yu y P. Goldman, «Rotor/seal experimental and analytical study on full annular rub,» *Journal of engineering for gas turbines and power. ASME,* vol. 124, nº April, 2002.

[7]. J. Yu, P. Goldman, D. Bently y A. Muszynska, «Rotor expirimental and analitical study on full annular rub,» *Journal of Engineering for Gas Turbines and Power. Transactions of the ASME,* vol. 124, 2002.

[8]. J. Lawen y G. Flowers, «Interation dynamics between a flexible rotor an auxiliary clearance bearing,» *ASME Journal of Vibration and Acoustics*, nº 121, pp. 183-189, 1999.

[9]. D. Bently, J. Yu y P. Goldman, «Full Annular Rub in Mechanical Seals,» *International Journal of Rotating Machinery*, vol. 8, nº 5, pp. 319-328, 2002.

[10]. A. Muszynska, «Misaligment Model,» Bently Rotor Dynamic Research Corporation. BRDRC Report No. 1, Minden, Nevada. USA, 1999.

[11]. A. Muszynska, «Misaligment model.,» Bently Rotor Dynamic Research Corporation., Minden, Nevada, 1999.

[12]. K. Kirk, «Evaluation of aerodynamic instability mechanims for rotor dynamics perfomance,» de *ASME 10th Biennal Conference on Mechanical Vibration and Noise. Paper nº 85-DET-147*, Cincinnati. United States., 1985.

[13]. Eungu, Park, Ypoung-Pil, Kim y A. Muszynska, «Identification of the quadrature resonances using modal nonsynchronous perturbation testing and dynamic stiffness approach for an anisotropic rotor system with fluid interaction,» *International Journal of Roating Machinery*, vol. 2, nº 3, pp. 187-199, 1996.

[14]. L. Tam, A. Przekwas, R. Hendricks y M. Braun, «Numerical and Analytical Study of Fluid Dynamic Forces in Seals and Bearings.,» *Journal of Vibration, Acoustics, Stress, and Reliability en Design. Trans of the ASME.*, vol. 110, nº 3, pp. 315-325, 1988.

[15]. F. Sorge, «Preventing the oil film instability in rotor-dynamics,» *Journal of Physics. Conference Series 744(1):012153*, 2016.

[16]. E. Jang, Y. Park, C. Kim y A. Muszyinska, «Identification of the quadrature resonances using modal nonsynchronous perturbation testing and dynamic stiffness approach for an anisotropic rotor system with fluid interaction,» *International Journal of Rotating Machinery*, vol. 2, nº 3, pp. 187-199, 1996.

[17]. A. Muszynska, «Whirl and whip-Rotor/bearing stability problems,» *Journal of Sound and Vibration*, vol. 110, nº 3, pp. 443-462, 1986.

[18]. L. Tam, A. Przekwas y R. Hendricks, «Numerical and Analytical Study of Fluid Dynamic Forces in Sealsand Bearing,» *Rotating Machinery Dynamics. ASME*, nº ASME Publ. H0400B, 1987.

[19]. B. Fraga, «Study of stability margin ans its connetion with the dynamic stiffness applied to a tidal turbine,» *International Journal of Latest Engineering Research and Applications (IJLERA)*, vol. 04, nº 01, 2019.

[20]. Y. Wang, X. Ren, X. Li y G. Chunwei, «Numerical investigation of subsynchronous vibration in floating ring bearings,» *Proceedings of the Institution of Mechanical Engineers Part J. Journal of Engineering Tribology 1994-1996*, Vols. %1 de %2208-210, 2018.

[21]. R. Hendricks y A. Muszynska, «Turbomachine sealing and secondary flows, part 2 – review of rotordynamics issues in inherently unsteady flow systems with small clearances,» de *Proceedings if the Second International Symposium on Stability Control of Rotating Machinery (ISCORMA-2)*, Gdansk, Poland, 2003.

[22]. P. Goldman y A. Muszynska, «Application of full spectrum to rotating machinery diagnostics,» *Orbit BNC*, vol. 20, nº 1, 1999.

